Available online at www.sciencedirect.com
SCIENCE DIRECT®
ELSEVIER
Mechatronics 14 (2004) 861–876
MECHATRONICS

Sliding mode based learning control for track-following in hard disk drives

W.C. Wu, T.S. Liu *

Department of Mechanical Engineering, National Chiao Tung University, 1001 Ta-Hsueh Road, Hsinchu 30010, Taiwan, ROC

Accepted 21 May 2004

Abstract

This study aims to develop a sliding mode based learning controller for track-following in hard disk drives. The proposed controller incorporates characteristics of sliding mode control into learning control. The reason for using sliding mode control is attributed to its robust properties dealing with model uncertainty and disturbances. The learning algorithm utilizes shape functions to approximate influence functions in integral transforms and estimate the control input to reduce repetitive error. Mathematical derivation of the control law and stability analysis are presented. To validate the proposed method, this work conducts track-following experiments.

Keywords: Sliding mode control; Learning control; Track-following control; Repetitive error

1. Introduction

The development of hard disk drive techniques has come to maturity. A pivoted voice coil motor (VCM) has been the common rotary actuator to perform track seeking and following in hard disk drives. While the hard disk drive data storage capacity and track density rapidly increase, repetitive disturbance degrades the track-following performance even more than before. Hence the control performance has to be elevated since the data track width and track pitch become smaller.

Disturbances in hard disk drive track-following motion can be classified into repetitive and nonrepetitive components. Nonrepetitive disturbances generally come

* Corresponding author. Fax: +886-3-5720634.
E-mail address: tsliu@mail.nctu.edu.tw (T.S. Liu).

0957-4158/$ - see front matter
doi:10.1016/j.mechatronics.2004.06.001

from the mechanical resonance, external impact, windage-induced disk flutter, etc. [1]. In addition, the repetitive disturbances mostly caused by the geometric bias of a disk, the relative position bias of the data track and rotary center, and the spindle motor defects [2]. In general, repetitive disturbances hurt track-following precision more than the nonrepetitive one [1,2]. In the conventional track-following control design, which only considers nominal plant models and nonrepetitive factors, such as PID, phase lead–lag, or notch filter can provide adequate gain and phase margin and reduce the resonance but can not perform well dealing with periodic disturbances [2]. Recently, many repetitive control methods have been proposed such as internal model type controllers [2], external model controller with a basis function algorithm [3] or with a learning algorithm [4]. These repetitive controllers can be categorized as internal mode based and external model based ones [5]. Controllers of internal model based are linear and constructed with a periodic signal generator inside a control loop. Conversely, external model based ones generate a cancellation signal outside the loop to eliminate the repetitive error. Comparison [5] of these methods indicates tradeoffs of error convergence speed and disturbance rejection ability. The internal model based approach with advantageous properties of linearity and easy analysis can converge rapidly but changes loop gains and influences sensitivity to disturbances. The robustness to unmodelled dynamics and noises is thus reduced. The external model controller is more complex in implementation. However, it applies a disturbance model outside the basic feedback loop, which can be adaptively adjusted to match the actual disturbance. Hence, the control compensation is more like a feedforward one that affects the nominal open loop gain less than the former.

Integrating the adaptive control [6] and learning control, the adaptive learning control [7] does not require exact knowledge of the plant model and can effectively eliminate the repetitive error after periods of learning. In addition, the nonlinear properties of plant and disturbance can be compensated by learning estimation [8]. It can be treated as a learning feedforward control, which is not designed completely prior to operation but keeps learning during control. Repetitive errors are compensated by a learning component that is operated in a feedforward path after training [9]. In addition, sliding mode control [10] has been developed and examined in various systems including nonlinear systems, discrete time systems, large scale systems, stochastic systems, multi-input, multi-output systems, etc. [11].

Dealing with model uncertainty and repetitive error motivates this work to integrate sliding mode control and learning control. As long as the error signal period is known in advance, without exact plant models the proposed sliding mode based learning controller can reduce repetitive error. The learning algorithm utilizes shape functions to approximate influence functions in integral transforms and estimate the control input to reduce repetitive error. Once the learning error converges, the sliding mode reaching condition [10,12] is obtained and the position error will converge to zero on a prescribed sliding surface.

This paper is organized as follows. Section 2 presents the sliding mode based learning control devoted to the repetitive tracking control. Some properties of the proposed controller are investigated. Section 3 describes a VCM model and simulation results. Experimental results are shown in Section 4.

2. Sliding mode based learning control

In this section, a sliding mode based learning controller is developed and its properties are presented.

2.1. Dynamic model and prescribed conditions

The equation of motion for an n-dimensional system can be expressed as

$$M(q)\ddot{q} + C(q,\dot{q})\dot{q} + G(q) = u \tag{1}$$

where $q(t)$, $\dot{q}(t)$, and $\ddot{q}(t)$ are respectively $n \times 1$ position, velocity, and acceleration vectors, u denotes a $n \times 1$ actuator input vector, $M(q)$ is a symmetric positive definite inertia matrix, $C(q,\dot{q})\dot{q}$ results from Coriolis and centripetal forces, and $G(q)$ is a gravitational force vector.

Define $\mathrm{Ker}(t,\tau)$ as a periodic Hibert–Schmit kernel function [8] that satisfies

$$\int_0^T \mathrm{Ker}(t,\tau)^2 \,\mathrm{d}\tau = \mathrm{ker} < \infty, \quad \mathrm{Ker}(t,\tau) = \mathrm{ker}(t+T,\tau) \geqslant 0$$

Condition 1. There exists an influence function $\alpha(\tau)$ such that

$$M(q)\dot{\upsilon} + C(q,\dot{q})\upsilon + G(q) = \int_0^T \mathrm{Ker}(t,\tau)\alpha(\tau)\,\mathrm{d}\tau \tag{2}$$

where $\upsilon(t) \in R^n$ is a vector function.

Condition 2. Using a proper definition of matrix $C(q,\dot{q})$, both $M(q)$ and $C(q,\dot{q})$ in Eq. (1) satisfy

$$q^{\mathrm{T}}(\dot{M} - 2C)q = 0 \quad \forall q \in R^n \tag{3}$$

That is, $(\dot{M} - 2C)$ is a skew-symmetric matrix. In particular, elements in $C(q,\dot{q})$ can be defined as

$$C_{ij} = \frac{1}{2}\left[\dot{q}^{\mathrm{T}}\frac{\partial M_{ij}}{\partial q} + \sum_{k=1}^{n}\left(\frac{\partial M_{ik}}{\partial q_j} - \frac{\partial M_{jk}}{\partial q_i}\right)\dot{q}_k\right].$$

2.2. Controller design

The present track-following control is to position a read/write head precisely at the center of desired tracks in the presence of disturbances. In order to deal with the periodic position error caused by repetitive disturbance, define periodic motion with a known period T as

$$q_{\mathrm{d}}(t+T) = q_{\mathrm{d}}(t), \quad \dot{q}_{\mathrm{d}}(t+T) = \dot{q}_{\mathrm{d}}(t), \quad \ddot{q}_{\mathrm{d}}(t+T) = \ddot{q}_{\mathrm{d}}(t)$$

where $q_{\mathrm{d}}(t)$, $\dot{q}_{\mathrm{d}}(t)$, and $\ddot{q}_{\mathrm{d}}(t)$ are desired position, velocity, and acceleration, respectively. For position output $q(t)$, the resultant position error is written as

$$e(t) = q(t) - q_{\mathrm{d}}(t) \tag{4}$$

Based on Condition 1, periodic motion corresponding to the reference velocity $\dot{q}_r$ can be written as

$$M(q)\ddot{q}_r + C(q,\dot{q})\dot{q}_r + G(q) = w = \int_0^T \mathrm{Ker}(t,\tau)\alpha(\tau)\,\mathrm{d}\tau \tag{5}$$

The reference velocity $\dot{q}_r$ is defined based on the adaptive control [13] as

$$\dot{q}_r(t) = \dot{q}_d(t) - \Lambda e(t) - \Gamma \int e(t)\,\mathrm{d}t \tag{6}$$

and the error between the output velocity and reference velocity is

$$\dot{e}_r(t) = \dot{q}(t) - \dot{q}_r(t) \tag{7}$$

Substituting Eq. (6) into (7) and employing Eq. (4) lead to

$$\dot{e}_r = \dot{q} - \left(\dot{q}_d - \Lambda e - \Gamma \int e\,\mathrm{d}t\right) = \dot{e} + \Lambda e + \Gamma \int e\,\mathrm{d}t$$

which implies that once the reference velocity error $\dot{e}_r$ equals zero, the system trajectory under control will satisfy

$$\dot{e}_r = \dot{e} + \Lambda e + \Gamma \int e\,\mathrm{d}t = 0$$

Concerning sliding mode control, to have the steady state position error stay on a sliding surface and consequently eliminate the position error [10], a sliding vector can be defined by letting $s = \dot{e}_r$ which leads to

$$s(t) = \dot{e}(t) + \Lambda e(t) + \Gamma \int e(t)\,\mathrm{d}t \tag{8}$$

where $\Lambda = \lambda_i I_d$ and $\Gamma = \gamma_i I_d$ are both positive definite matrices, and I_d represents the identity matrix. Hence, this study defines a control input u_{SMLC} that integrates an estimated learning compensation used to approximate w in Eq. (5), a proportional, integral, and derivative (PID) feedback control term, and a discontinuous control term; i.e.

$$\begin{aligned} u_{SMLC} &= \tilde{w} - K_I \int e\,\mathrm{d}t - K_P e - K_D \dot{e} - Q\,\mathrm{sgn}(\dot{e}_r) \\ &= \tilde{w} - K_D\left(\dot{e} + K_D^{-1}K_P e + K_D^{-1}K_I \int e\,\mathrm{d}t\right) - Q\,\mathrm{sgn}(s) \end{aligned} \tag{9}$$

Denoting $\Lambda = K_D^{-1}K_P$ and $\Gamma = K_D^{-1}K_I$ and substituting Eq. (8) into (9) yield

$$u_{SMLC} = \tilde{w} - Ks - Q\,\mathrm{sgn}(s) \tag{10}$$

where Q and $K = K_D = kI_d$ are both positive definite matrices. The control block diagram is shown in Fig. 1.

Different from conventional controllers designed based on nominal plant models, the proposed controller Eq. (10) does not require exact knowledge of plant and

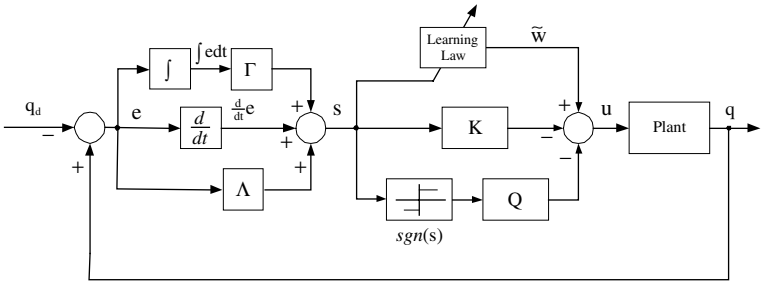

Fig. 1. System block diagram.

disturbance models. The three terms in Eq. (10) are correlated based on Eqs. (5), (6) and (8). It will be proved in Section 2.3 that the proposed controller after learning will constitute an equivalent sliding mode controller that satisfies the sliding mode reaching condition i.e. making the tracking error trajectory approach and stay on a prescribed sliding surface. Accordingly, the proposed controller with properties of both learning control and sliding mode control can be carried out doing without complicated procedure and any plant model. To verify stability of the proposed controller, a mathematical proof is given in the following section. Moreover, the reaching condition for the sliding mode control is also verified.

Based on the learning control [7], the desired input $\tilde{w}$ can be estimated as

$$\tilde{w}(t) = \int_0^T \mathrm{Ker}(t,\tau)\widetilde{I}(t,\tau)\,\mathrm{d}\tau \tag{11}$$

where $\widetilde{I}(t,\tau)$ is the unknown estimated influence function.

Definition: Let $C_k(T)$ denote a subset of $C(T)$ (which is the space of continuous T-period functions $I(\bullet): R_+ \to R^n$) such that every $I(\bullet)$ is piecewise continuously differentiable, and

$$\sup_{t\in[0,T]}\left|\frac{\mathrm{d}}{\mathrm{d}t}I(\bullet)\right| \leqslant k$$

Given a collection for shape functions $\{\Phi_i\}$ and $\phi > 0$, there exist a finite number of shape functions $\{\Phi_0, \Phi_1, \Phi_2, \ldots, \Phi_N\}$ that uniformly approximate members of $C_k(T)$ within $\phi > 0$, i.e. for every $I \in C_k(T)$, there exist constant vectors $C_0, C_1, C_2, \ldots, C_n \in R^n$ such that

$$\sup_{t\in[0,T]}\left|I(t) - \sum_{i=0}^{N} C_i\Phi_i\right| < \phi$$

To estimate the desired influence function $I(t)$, it can be approximated by a linear combination of shape functions Φ_i. Hence,

$$I(t) \cong \sum_{i=0}^{N} C_i\Phi_i(t)$$

where $C_i \in R^n$ represent unknown coefficient vectors for each shape function Φ_i at an instant, and $N+1$ denotes the total number of shape functions. Hence, the estimated term is generated by determining coefficients $\widetilde{C}_i$, i.e.,

$$\widetilde{I}(t,\tau) = \sum_{i=0}^{N} \widetilde{C}_i(t,\tau)\Phi_i(\tau) \tag{12}$$

where $\widetilde{C}_i(t,\tau)$ are estimated corresponding coefficients. In addition, the sliding vector is introduced into an adaptation law as

$$\frac{\partial}{\partial t}\widetilde{C}_i(t,\tau) = -K_L \,\mathrm{Ker}(t,\tau)\Phi_i(\tau)s \tag{13}$$

where the learning gain $K_L = k_l I_\mathrm{d}$ is a symmetric positive definite matrix.

This study employs a set of piecewise linear functions, as depicted in Fig. 2. Accordingly, in each interval of $[iT/N, (i+1)T/N]$, only two linear shape functions,

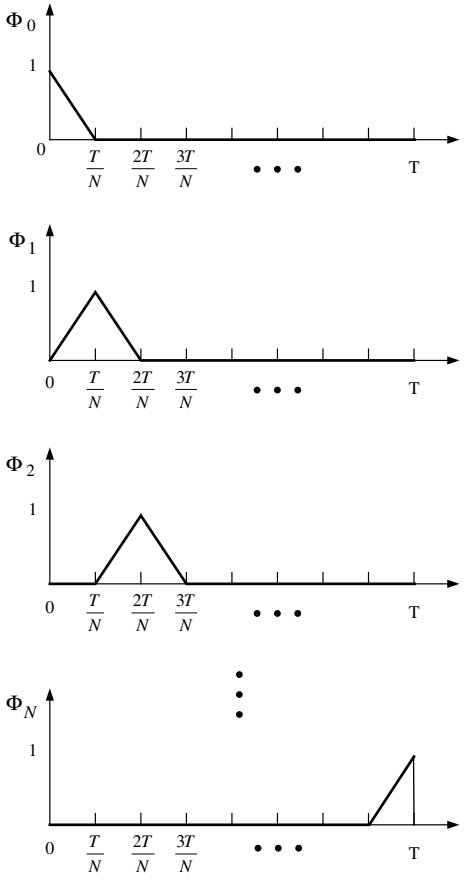

Fig. 2. Piecewise linear shape functions.

Φ_i and Φ_{i+1}, are required; i.e. there are only two corresponding coefficients, c_i and c_{i+1}, to be updated at any instant. The linear shape functions are a B-spline set of second order. A B-spline of order n consists of piecewise polynomial functions of order $n-1$. The time span of each shape function is defined as its support. If there are $N+1$ equally spaced shape functions, the period can be expressed by

$$T = Nd/2 \tag{14}$$

where d is the shape function support. It in general can be regarded as a filter as shown in Fig. 3 with $N = 5$, for example. The accuracy of the filtering or called approximating process depends on the support of the shape functions [14]. For ease of computing kernel functions, piecewise linear functions shown in Fig. 4 are used as kernel functions for integral transforms, where the span 'sp' denotes a subinterval length.

2.3. Stability analysis

Applying the control input given by Eq. (10) into the system in Eq. (1), system dynamics subject to the present controller is written as

$$M(q)\ddot{q} + C(q,\dot{q})\dot{q} + G(q) = \tilde{w} - Ks - Q\,\mathrm{sgn}(s)$$

The approximation error $\bar{w} = \tilde{w} - w$ of control inputs between Eqs. (5) and (11) can be written as

$$\begin{aligned}\bar{w} = \tilde{w} - w &= \int_0^T \mathrm{Ker}(t,\tau)\tilde{I}(t,\tau)\,\mathrm{d}\tau - \int_0^T \mathrm{Ker}(t,\tau)\alpha(\tau)\,\mathrm{d}\tau \\ &= [M(q)\ddot{q} + C(q,\dot{q})\dot{q} + G(q) + Ks + Q\,\mathrm{sgn}(s)] - [M(q)\ddot{q}_\mathrm{r} + C(q,\dot{q})\dot{q}_\mathrm{r} + G(q)] \\ &= M(q)\dot{s} + C(q,\dot{q})s + Ks + Q\,\mathrm{sgn}(s)\end{aligned} \tag{15}$$

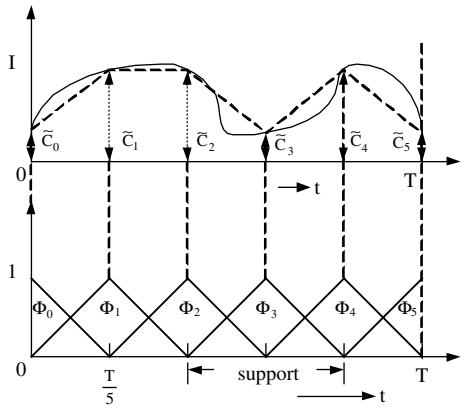

Fig. 3. The influence function approximating process by shape functions with the shape functions number of $N = 5$.

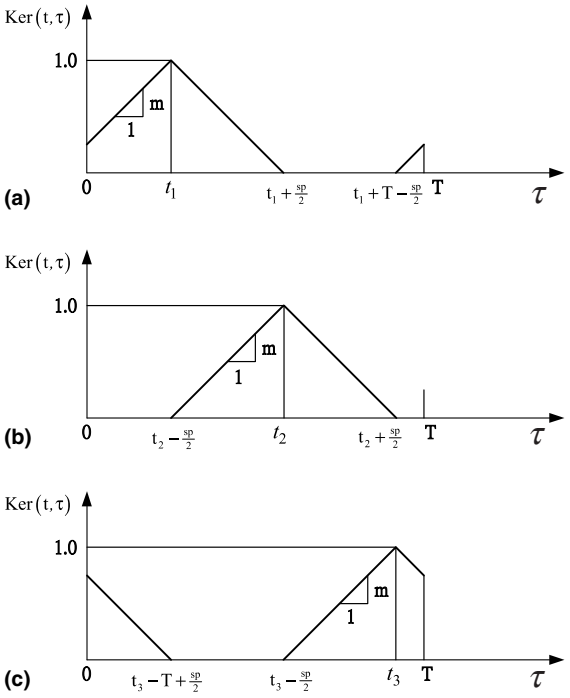

Fig. 4. Piecewise linear kernel functions. (a) $0 < t_1 < \frac{sp}{2}$, (b) $\frac{sp}{2} < t_2 < T - \frac{sp}{2}$, (c) $T - \frac{sp}{2} < t_3 < T$.

Taking the time derivative of Eq. (15) leads to

$$\dot{\bar{w}} = \ddot{\bar{w}} - \dot{w}$$

It follows from Eqs. (11)–(13) that

$$\dot{\bar{w}} = \frac{\partial}{\partial t}\left[\int_0^T \mathrm{Ker}(t,\tau)\widetilde{I}(t,\tau)\,\mathrm{d}\tau - \int_0^T \mathrm{Ker}(t,\tau)\alpha(\tau)\,\mathrm{d}\tau\right] = -K_L Z(\mathrm{Ker},\Phi)s \tag{16}$$

where $Z(\mathrm{Ker},\Phi)$ is a function of the kernel function and the shape function.

In order to verify stability of the proposed control method, i.e. $s = \dot{e}_r$ asymptotically converges to zero, prescribe a Lyapunov function candidate of the form

$$V = \tfrac{1}{2}(s^{\mathrm{T}}Ms + \bar{w}^{\mathrm{T}}K_L\bar{w}) \geqslant 0 \tag{17}$$

Taking the time derivative of V leads to

$$\dot{V} = \tfrac{1}{2}s^{\mathrm{T}}\dot{M}s + s^{\mathrm{T}}M\dot{s} + \bar{w}^{\mathrm{T}}K_L\dot{\bar{w}} \tag{18}$$

From Eq. (15),

$$M(q)\dot{s} = \bar{w} - C(q,\dot{q})s - Ks - Q\,\mathrm{sgn}(s)$$

Hence, Eq. (18) can be rewritten as

$$\dot{V} = \tfrac{1}{2}s^{\mathrm{T}}\dot{M}s + s^{\mathrm{T}}[\bar{w} - C(q,\dot{q})s - Ks - Q\,\mathrm{sgn}(s)] + \bar{w}^{\mathrm{T}}K_L\dot{\bar{w}}$$
$$= \tfrac{1}{2}s^{\mathrm{T}}(\dot{M} - 2C)s + s^{\mathrm{T}}[\bar{w} - Ks - Q\,\mathrm{sgn}(s)] + \bar{w}^{\mathrm{T}}K_L\dot{\bar{w}}$$

Applying Condition 2, it becomes

$$\dot{V} = s^{\mathrm{T}}[\bar{w} - Ks - Q\,\mathrm{sgn}(s)] + \bar{w}^{\mathrm{T}}K_L\dot{\bar{w}}$$

Substituting Eq. (16) into the above equation leads to

$$\dot{V} = s^{\mathrm{T}}[\bar{w} - Ks - Q\,\mathrm{sgn}(s)] - \bar{w}^{\mathrm{T}}K_L^2 Z(\mathrm{Ker}, \Phi)s$$
$$= s^{\mathrm{T}}[I_{\mathrm{d}} - K_L^2 Z(\mathrm{Ker}, \Phi)]\bar{w} - s^{\mathrm{T}}Ks - s^{\mathrm{T}}Q\,\mathrm{sgn}(s) \tag{19}$$

Assuming that both $\bar{w}$ and $Z(\mathrm{Ker}, \Phi)$ are bounded, i.e. $\|\bar{w}\| \leqslant \overline{W}$ and $\|Z(\mathrm{Ker}, \Phi)\| \leqslant \zeta$, where $\overline{W}$ and ζ are positive, one has

$$\|[I_{\mathrm{d}} - K_L^2 Z(\mathrm{Ker}, \Phi)]\bar{w}\| \leqslant \|I_{\mathrm{d}} - K_L^2 Z(\mathrm{Ker}, \Phi)\|\left\|\bar{w}\right\|$$
$$\leqslant [\|I_{\mathrm{d}}\| + \|K_L^2 Z(\mathrm{Ker}, \Phi)\|]\|\bar{w}\| \leqslant (1 + k_l^2\zeta)\overline{W} \tag{20}$$

Eq. (19) can be rewritten as

$$\dot{V} = s^{\mathrm{T}}\{[I_{\mathrm{d}} - K_L^2 Z(\mathrm{Ker}, \Phi)]\bar{w} - Q\,\mathrm{sgn}(s)\} - s^{\mathrm{T}}Ks$$

Hence, letting $Q[(1 + k_l^2\zeta)\overline{W} + \delta]I_{\mathrm{d}}$ and applying Eq. (20) yields

$$\dot{V} \leqslant -\delta\|s\| - k\|s\|^2 \tag{21}$$

where $\delta > 0$. Since $V > 0$ from Eq. (17) and according to Eq. (21), the negative definiteness of $\dot{V}$ implies the convergence of s. In addition, a finite reaching time to the sliding surface $s = 0$ is ensured by designing $\delta \geqslant \eta$. Hence, the reaching condition [12,15]

$$\dot{V} \leqslant -\eta\|s\|, \quad \eta > 0$$

for the sliding mode control is ensured. As a consequence, the position error will converge to zero on the sliding surface $s = \dot{e} + \Lambda e + \Gamma\int e\,\mathrm{d}t = 0$.

3. Plant model and simulation results

Since hard disk drives employ a pivoted VCM as the track seeking and following actuator, in this study the control performance is investigated with a VCM plant model whose parameters were identified and listed in Table 1 [16]. The identified plant model is adopted to perform simulation. The nominal plant model is defined as

$$\frac{Q(s)}{U(s)} = P_{\mathrm{VCM}}(s) = k\left(\frac{1}{s^2} + \sum_{i=1}^{2}\frac{\gamma_i}{s^2 + 2\zeta_i\omega_i s + \omega_i^2}\right)\mathrm{e}^{-T_{\mathrm{d}}S} \tag{22}$$

where $q(t)$ denotes the position output (μm) of the pickup head, $u(t)$ is the input current (A), k is a constant gain, ζ_i, γ_i, and ω_i are ith mode damping factor, residue

Table 1
VCM model parameters

F_s	Sampling frequency	11 kHz
ω_1	First resonant frequency	5200 Hz
ω_2	Second resonant frequency	6100 Hz
ζ_1	First resonant damping factor	0.02
ζ_2	Second resonant damping factor	0.01
γ_1	Residue of first resonant mode	−1.2
γ_2	Residue of second resonant mode	−0.2
K	Constant gain	1.3×10^8
T_d	Time delay including ZOH effect	88 μs

and resonant frequency, respectively, and T_d is a time delay. The time delay includes the effect of delay caused by zero order hold (ZOH), which is half of the sampling period. The term of the time delay is approximated by a third-order Padé approximation [17].

To demonstrate the periodic disturbance rejection of the track-following control with the proposed controller, a input periodic disturbances is applied as a composite sinusoidal signal consisting of multiple frequencies of $\omega = 60$ Hz. Thus, the control input disturbance d_I is expressed as

$$d_I(t) = 0.01 \times [0.1 + \sin(2\pi\omega t) + 0.5\sin(4\pi\omega t) + 0.25\sin(8\pi\omega t)](A) \tag{23}$$

In order to evidence the periodic error convergence capability, a PD controller is used to compare with the proposed controller. It can be found from Fig. 1 that the proposed controller without the learning control and the discontinuous switching terms is equivalent to a PD controller based on the sliding variable definition

$$s(e) = \dot{e} + \Lambda e$$

Hence, the equivalent PD controller can be rewritten as

$$u_{PD} = -Ks = -K(\dot{e} + \Lambda e) = -K_D\dot{e} - K_P e$$

where $K_D = K$ and $K_P = K\Lambda$ are corresponding PD control gains. The corresponding controller gains in both controllers will be the same in the discrete time simulation at 100 kHz sampling rate for impartial comparison. Assuming the repetitive tracking error is caused by a periodic input disturbance, Figs. 5 and 6 compare repetitive errors in amplitudes and power spectrums between both control methods, respectively, where the PD controller cannot cope with the disturbance. By contrast, using the proposed controller, the repetitive tracking error caused by the input disturbance is eliminated after five learning periods. The power spectrum in Fig. 6 shows that error component due to fundamental frequency $\omega = 60$ Hz has been removed.

Furthermore, this study superimposes a white noise of zero mean and variance 5 mA on a periodic input disturbance and another white noise of zero mean and variance 2 μm in the position measurement to examine the learning control robustness to nonrepetitive disturbances. Fig. 7 shows that the proposed controller is robust in the presence of white noise and the repetitive error convergence capability is not degrade at all. At a lower sampling frequency of 1 kHz, Fig. 8 indicates the

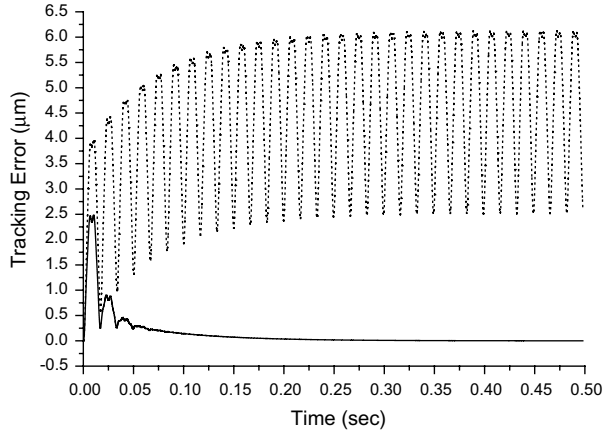

Fig. 5. Tracking error amplitudes of sliding mode based learning control (solid line) and PD control (dotted line) under periodic input disturbances.

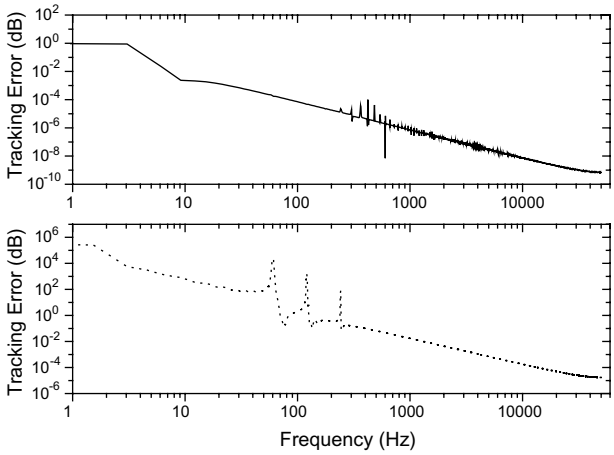

Fig. 6. Tracking error power spectrums of sliding mode based learning control (solid line) and PD control (dotted line) under periodic input disturbances.

repetitive error convergence conditions subject to different disturbance frequencies, where the lower the disturbance frequency is, the faster the tracking error converges.

4. Experiment and results

As shown in Fig. 9, this experimental setup contains a VCM that drives a suspension arm in a 3.5" hard disk drive. For the position sensing purpose, this study

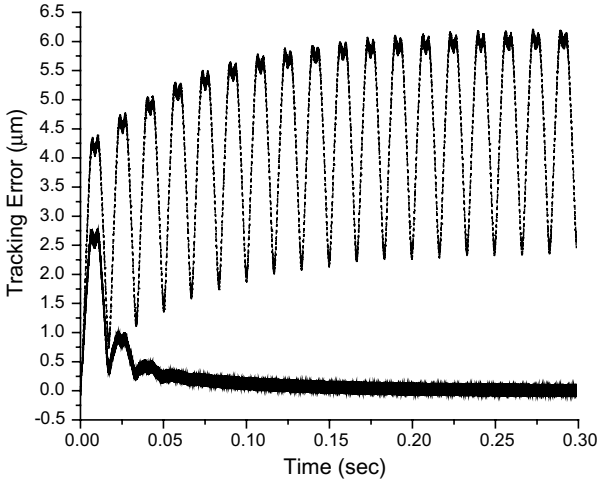

Fig. 7. Tracking errors of sliding mode based learning control (solid line) and PD control (dotted line) subject to white noise in both control input and measurement signal.

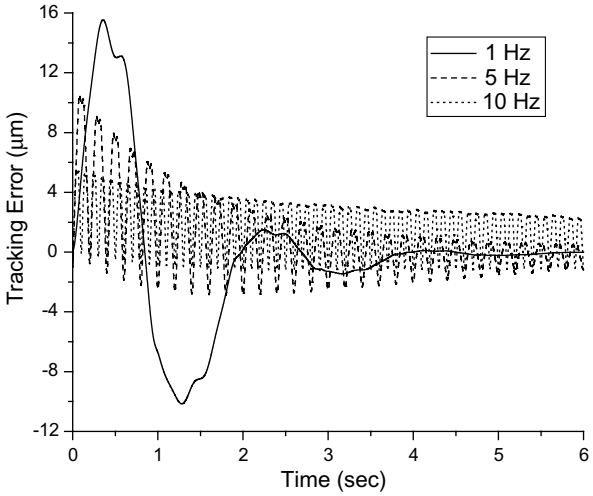

Fig. 8. Tracking error of sliding mode based learning control subject to various frequencies of periodic

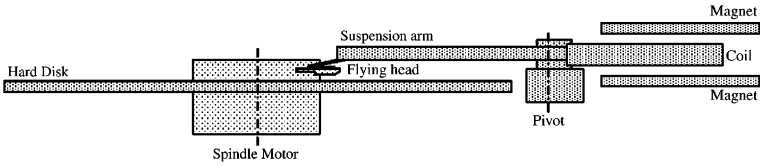

Fig. 9. VCM rotary actuator in hard disk drive system.

uses a Renishaw RGH22S digital optical readhead and a fan-shaped component with a reflective tape scale attached at the tip of the suspension arm, as shown in Fig. 10. The reflective tape scale is scanned by a digital optical readhead. The readhead generates a digital square wave signal, which is encoded in a NI PCI-7344 Flex-Motion control card as position feedback signals. Accordingly, the positioning resolution can achieve 0.1 μm.

Fig. 11 depicts this experimental setup. It consists of a Pentium II PC to perform control algorithm calculation at 1 kHz sampling rate that is the same as simulation, a motion control card to encode the digital square wave signal and convert digital control signal to analog output, an amplifier to drive the VCM, and a modified VCM with the suspension arm as the control plant.

To validate the controller proposed in this work, experimental results of both equivalent PD controller and sliding mode based learning controller are compared. In practice, the repetitive position error is caused by spindle motor bias, disk runout and deformation, etc. As long as the period of the disturbance is known, the present method can eliminate the repetitive error. Further, the periodic disturbance prescribed in Eq. (23) is included on purpose in the control input. Repetitive errors of PD control and sliding mode based learning control are compared in Fig. 12, where in the presence of 1 Hz disturbance the proposed method outperforms the PD control. Tracking results compared with those of 5 and 10 Hz disturbances are presented in Fig. 13. The learning performance with a fixed learning gain degrades with increasing disturbance frequency due to sampling rate limitation of the controller hardware.

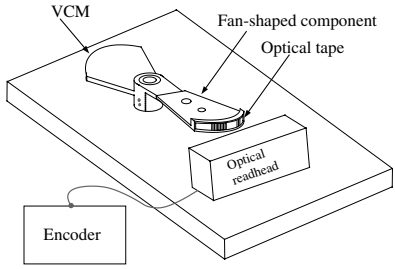

Fig. 10. Measurement device.

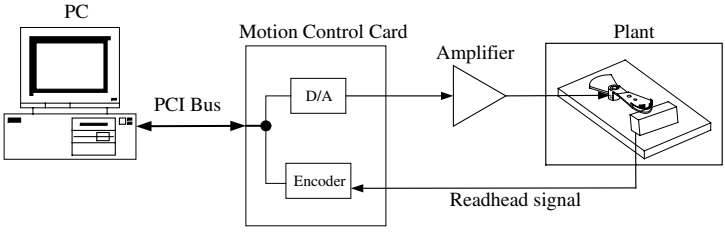

Fig. 11. Experimental setup.

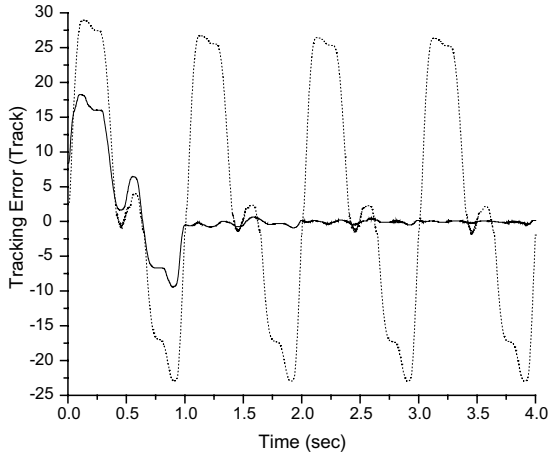

Fig. 12. Experimental results in sliding mode based learning control (solid line) and PD control (dotted line).

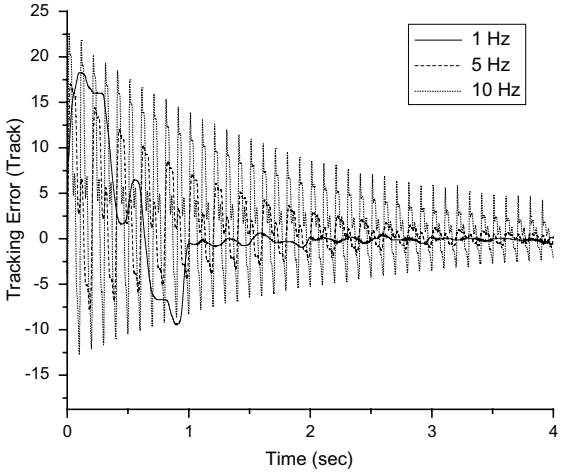

Fig. 13. Experimental results of sliding mode based learning control among different frequencies of disturbances.

Modern disk drives have much higher spin speed, say 12,000 rpm that causes a 200 Hz high frequency disturbance. To deal with a higher frequency disturbance, using hardware of higher sampling rate to implement the proposed controller will be an effective solution. In tracking sinusoidal signals, the total number N of shape functions in a learning period T determines error magnitudes in steady state. Since the number N of shape functions is prescribed as 100 in experiments that result in Fig. 13, to obtain comparable performance in dealing with a 200 Hz disturbance of

period $T = 5$ ms, it is also prescribed that $N = 100$. Substituting $T = 5$ ms and $N = 100$ into Eq. (14) gives $d = 0.1$ ms. However, according to the last paragraph in Section 2.2, the shape function support d of a piecewise linear shape function as shown in Fig. 2 has to be at least twice the sampling period Δt to implement the proposed controller in discretized form. Hence, $\Delta t = 0.05$ ms; i.e. the sampling rate must be at least 20 kHz. An alternative is to use other shape functions such as Fourier series bases [4] that may better approximate the desired input even at a low sampling rate, which however will increases computation time.

5. Conclusion

A sliding mode based learning control method has been proposed for a VCM in hard disk drives to perform disturbance rejection in track-following control. Mathematical derivation of the control law and stability proof have been carried out. According to experimental results, without an exact plant model the proposed control method achieves rejection of periodic disturbances. Additionally, the sliding mode based learning control not only exhibits error convergence faster than the PD control but also can eliminate the repetitive error. However, in experiments due to time delay caused by I/O, the sampling rate is confined to 1 kHz at most. The tracking error can be reduced more effectively with lower frequency disturbance signals or using higher sampling rate if available. The latter can be achieved by using more advanced control hardware.

Acknowledgements

This work was supported by 'Photonics science and technology for tera era', Center of Excellence, Ministry of Education, Taiwan under Contract 89-E-FA06-1-4.

References

[1] Atsumi T, Arisaka T, Shimizu T, Yamaguchi T. Vibration servo control design for mechanical resonant modes of a hard disk drive actuator. JSME Int J C: Mech Syst Mach Elements Manuf 2003;46(3):819–27.
[2] Chew K, Tomizuka M. Digital control of repetitive errors in disk-drive systems. IEEE Control Syst Mag 1990;10:16–20.
[3] Tomizuka M, Kempf C. Design of discrete time repetitive controllers with applications to mechanical system. In: Proceeding of 11th International Federation of Automatic Control World Congress, Tallinn, Estonia, USSR, 1990. p. 5.
[4] Cao WJ, Xu JX. Fourier series-based repetitive learning variable structure control of hard disk drive servos. IEEE Trans Magn 2000;36(5):2251–4.
[5] Kempf C, Messner W, Tomizuka M, Horowitz R. Comparison of four discrete-time repetitive control algorithm. IEEE Control Syst Mag 1993;13(6):48–54.
[6] Sadegh N, Horowitz R. Stability and robustness analysis of a class of adaptive controllers for robotic manipulators. Int J Robotics Res 1990;9(3):74–92.

[7] Sadegh N, Guglielmo K. A new repetitive controller for mechanical manipulators. J Robotic Syst 1990;8(4):507–29.
[8] Messner W, Horowitz R, Kao W, Boals M. A new adaptive learning rule. IEEE Trans Automatic Control 1991;36(2):188–97.
[9] Velthuis WJR, de Vries TJA, Schaak P, Gaal EE. Stability analysis of learning feedforward control. Automatica 2000;36(12):1889–95.
[10] Utkin VI. Sliding modes in control optimization. New York: Springer-Verlag; 1992.
[11] Hung JY, Gao WB, Hung JC. Variable structure control: a survey. Special Issue on Sliding Mode Control. IEEE Trans Ind Electron 1993;40(1):2–22.
[12] Bailey E, Arapostathis A. Simple sliding mode control scheme applied to robot manipulators. Int J Control 1987;45(4):1197–209.
[13] Slotine JJE, Li W. On the adaptive control of robot manipulators. Int J Robotics Res 1987;6(3):49–59.
[14] Velthuis WJR, de Vries TJA, Gaal EE. Experimental verification of the stability analysis of learning feedforward control. In: Proceedings of the 37th IEEE International Conference on Decision and Control, Florida, USA, December 16–18, 1998. p. 1225–9.
[15] Slotine JJE, Coetsee JA. Adaptive sliding controller synthesis for non-linear systems. Int J Control 1986;43(6):1631–51.
[16] Ohno K, Abe Y, Maruyama T. Robust following control design for hard disk drives. In: Proceedings of the IEEE International Conference on Control Applications, Mexico City, Mexico, September 5–7, 2001. p. 930–5.
[17] Golub GH, Van Loan CF. Matrix computations. Baltimore: Johns Hopkins University Press; 1989. p. 557–8.